FREE-FREE ABSORPTION ON PARSEC SCALES IN SEYFERT GALAXIES.

A. L. ROY[a](aroy@mpifr-bonn.mpg.de)
J. S. ULVESTAD[b]
A. S. WILSON[c]
E. J. M. COLBERT[d]
C. G. MUNDELL[e]
J. M. WROBEL[b]
R. P. NORRIS[f]
H. FALCKE[a] and T. KRICHBAUM[a]

Seyfert galaxies come in two main types (types 1 and 2) and the difference is probably due to obscuration of the nucleus by a torus of dense molecular material. The inner edge of the torus is expected to be ionized by optical and ultraviolet emission from the active nucleus, and will radiate direct thermal emission (e.g. NGC 1068) and will cause free-free absorption of nuclear radio components viewed through the torus (e.g. Mrk 231, Mrk 348, NGC 2639). However, the nuclear radio sources in Seyfert galaxies are weak compared to radio galaxies and quasars, demanding high sensitivity to study these effects. We have been making sensitive phase referenced VLBI observations at wavelengths between 21 and 2 cm where the free-free turnover is expected, looking for parsec-scale absorption and emission. We find that free-free absorption is common (e.g. in Mrk 348, Mrk 231, NGC 2639, NGC 1068) although compact jets are still visible, and the inferred density of the absorber agrees with the absorption columns inferred from X-ray spectra (Mrk 231, Mrk 348, NGC 2639). We find one-sided parsec-scale jets in Mrk 348 and Mrk 231, and we measure low jet speeds (typically $\leq 0.1c$). The one-sidedness probably is not due to Doppler boosting, but rather is probably free-free absorption. Plasma density required to produce the absorption is $N_{\rm e} \geq 2 \times 10^5$ cm^{-3} assuming a path length of 0.1 pc, typical of that expected at the inner edge of the obscuring torus.

1 Introduction

Sensitivity of VLBI is constantly improving, and the recent advent of routine phase referencing with the VLBA has made the imaging of many radio-quiet active galaxies possible. These are mostly too weak for self-calibration, having only a few or tens of mJy core flux density, so we have now been exploiting phase referencing to make systematic surveys of Seyfert galaxies with milliarcsecond (mas) resolution, at multiple frequencies to image the nuclear radio structures and to measure core spectra and jet speeds.

Historically, the torus proposed by Seyfert unification schemes was invoked to explain why we do not see the broad-line region (BLR) in Sy 2 nuclei that is thought to be present in most Seyferts. (The BLR is seen indirectly in some narrow-line Seyferts through scattering into our line of sight, or by IR spectroscopy that penetrates the obscuring dust.) Recently, direct evidence for the existence of this torus has come from VLBA images of H_2O maser discs in NGC 4258 [1], and NGC 1068 [2], and images of possible thermal emission from the ionized inner edge of the torus in NGC 1068 [3]. Though masers provide a lot of information (e.g. $M_\bullet$, $L/L_{\rm edd}$), unfortunately they are rare because their existence requires special geometry and conditions. On the other hand, free-free effects due to the ionized inner edge of an obscuring torus should be common and should produce characteristic spectral shapes and

[a]Max-Planck-Institut für Radioastronomie, Auf dem Hügel 69, D-53121 Bonn, Germany
[b]National Radio Astronomy Observatory, P.O. Box O, Socorro, NM 87801, USA
[c]University of Maryland, and Space Telescope Science Institute. Address: Department of Astronomy, University of Maryland, College Park, MD 20742, USA
[d]Goddard Space Flight Center, Mail Code 662, Laboratory for High Energy Astrophysics, NASA Goddard Space Flight Center, Greenbelt, DM 20771, USA
[e]Department of Astronomy, University of Maryland, College Park, MD 20742, USA
[f]Australia Telescope National Facility, P.O. Box 76, Epping NSW 1710, Australia

one-sided jets and thermal emission that we can look for using multi-frequency VLBI imaging.

2 Expected Torus Structure

The torus structure is usually modelled as a slab of gas irradiated from one side with X-rays from the AGN (e.g. [4, 5]). The predicted temperature and chemical abundances vary with depth into the slab as the shielding increases, and in a typical model, the inner edge of the slab lies ~ 0.3 pc from the AGN [6] and the slab is fully ionized for a depth of 0.1 pc at a temperature of 10^4 K and density of a few$\times 10^4$ cm^{-3}. Such a plasma would have an optical depth due to free-free absorption of unity at 5 GHz, or higher if the density is higher or the path length is longer. Going deeper into the slab the material is warm (6000 K) atomic and then cool (600 K) molecular, where the maser emission is produced.

Thus, if we view an edge-on torus around an AGN with a core-jet radio source, the core spectrum should be absorbed and the jet should be progressively less absorbed along its length like in Cyg A [7].

3 The Surveys

We selected eight nearby Seyfert galaxies that were known to have strong radio cores in existing VLA or VLBI images. We observed three type 1 Seyferts (NGC 4151, NGC 7469, Mrk 231) and five type 2 Seyferts (NGC 1068, NGC 2639, NGC 5506, Mrk 348 and Mrk 463) with the VLBA between 1996 and 1998 at three frequencies out of 1.6 GHz, 4.8 GHz, 8.4 GHz, and 15 GHz (depending on the source strength), chosen to span either side of the expected free-free absorption peak. The VLBA beamwidth at 1.6 GHz was 5 mas and we tapered the array at higher frequencies for measuring spectral indices. We integrated for 1 h per source per frequency, over a range of position angles. We observed a phase referencing calibrator every 2 to 10 min, depending on the frequency, to remove atmospheric and instrumental phase variations. Self-calibration then proved able to remove remaining phase errors and improved the fidelity of the final images. These were typically thermal noise limited, at a 5-σ level of 2 mJy beam^{-1} in a 2 mas beam (35×10^6 K) at full resolution at 5 GHz, or 1.0×10^6 K when tapered to 13 mas resolution for surface brightness sensitivity.

We have also conducted a search for further examples of thermal emission from the ionized inner edge of the accretion disc by making deep integrations at 8.4 GHz with the VLBA on five Seyfert galaxies known to contain flat-spectrum radio cores (T0109-383, NGC 2110, NGC 5252, Mrk 926, and NGC 4388). The beamsize was 2 mas, and integration times of 2.5 to 6 h yielded thermal-noise-limited images with sensitivity of 3-$\sigma = 10^6$ K, sufficient to detect an accretion disc like that in NGC 1068.

3.1 Results 1: The Core Spectra

Radio cores in Seyferts typically produce optically-thin synchrotron emission with $S \sim \nu^{-0.7}$ when imaging with resolution of 100 to 1000 pc [9]. We found similar results at 0.1 to 1 pc resolution, with most components showing steep power-law spectra. However, a number of Seyferts also showed a flat or absorbed spectrum in at least one nuclear component. The clear cases are shown in Fig 1.

Such absorption could in principle be caused by synchrotron self absorption (SSA), Razin-Tsytovich suppression, or free-free absorption. The Razin-Tsytovich effect is unlikely because it requires field strengths of 10^{-4} gauss for a 0.1-pc absorber, which is 1000 times below equipartition.

Synchrotron self-absorption requires high brightness temperatures. For comparison, in NGC 1068, although the AGN component (S1) has a spectrum of $\nu^{+0.3}$ around 5 GHz, it is resolved, with $T_{\rm b}$ of 4×10^6 K [3], which is too low to be caused by SSA (unless scattering has enlarged the source) and so the rising spectrum is more naturally accounted for as thermal emission. In NGC 4151, the nucleus probably contains a flat-spectrum component, and we find $T_{\rm b} < 1.1 \times 10^7$ K to $> 3.2 \times 10^7$ K at 4.8 GHz for the jet and core components. The upper range of $T_{\rm b}$ is a lower limit because the component E2 is unresolved, so the temperature could in principle be $> 10^{10}$ K, high enough for SSA. Alternatively, the flat-spectrum contribution to the nuclear flux could be due to free-free absorption by

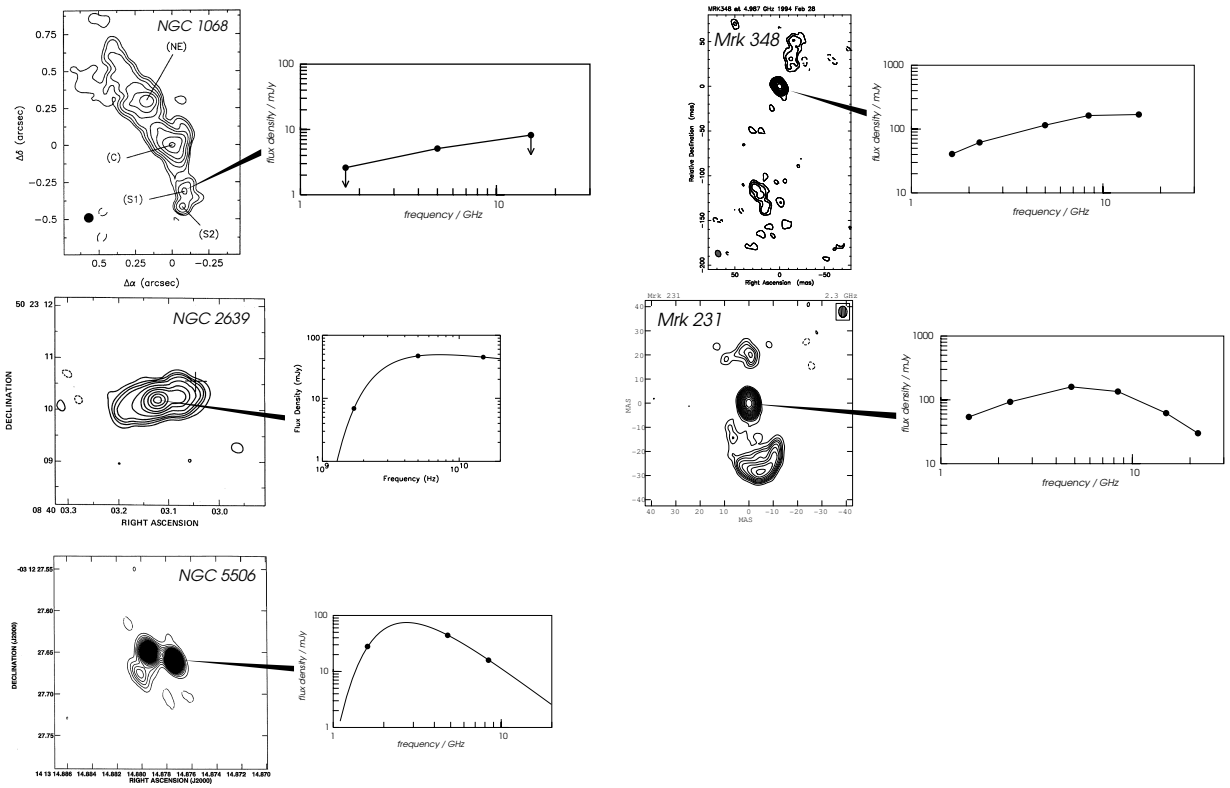

Figure 1: The five Seyfert galaxies that show absorbed spectra in their nuclear components. Anticlockwise from top left: NGC 1068, MERLIN 6 cm image from [10], and our VLBA spectrum [11]; NGC 2639, VLA image from [9], and our spectrum [12]; NGC 5506 image and spectrum from our VLBA survey; Mrk 231 image at 13 cm and spectrum from [13]; Mrk 348 imaged by us at 6 cm with a global VLBI array [14], and spectrum from [15].

the inner part of an HI disc that has been seen in absorption by [16]. NGC 2639 contains an unresolved and variable radio core with an absorbed spectrum peaking around 5 GHz. The brightness temperature is $> 1.0 \times 10^9$ K at 5 GHz, and so could be SSA. However, this is also a water maser galaxy, indicating the presence of an edge-on disc through which we probably view the radio core. The inner edge of the disc should be ionized and should cause free-free absorption of the nuclear continuum as seen. Mrk 348 and Mrk 231 both have nuclear radio components with absorbed spectra [13, 15]. Brightness temperatures are $> 7 \times 10^9$ K (Mrk 348) and $> 6 \times 10^9$ K (Mrk 231), which could be SSA or free-free absorption. Free-free absorption also could account for the absence of counter-jets (next section).

3.2 Results 2: One-Sided Jets

Mrk 348 and Mrk 231 both show a core and two-sided ejection on 50-pc scales, and high-resolution 15-GHz images resolve the cores into 0.5-pc doubles. Presumably, one component is the core, and the other is a jet on one side. A counter-jet is not seen in either object.

The lack of a counter-jet is usually due to Doppler boosting, but here the jet probably lies across our line of sight [17], and component speeds are low (below). Instead, free-free absorption of the counter-jet in an ionized disc around the AGN is the most natural explanation for the apparent one-sidedness.

Indeed, the X-ray absorbing column towards Mrk 348 is 10^{23} cm^{-2} [18], and towards Mrk 231 is 6×10^{22} cm^{-2} [19], which, if distributed over a path of 0.1 pc like the inner edge of the torus corresponds to densities of $2 - 3 \times 10^5$ cm^{-3}, enough to produce free-free absorption of the counter jet.

Interestingly, three Seyferts in our sample are water-maser sources (NGC 1068, NGC 2639, and NGC 5506) indicating an edge-on disc, and all are Seyfert 2 galaxies and show absorbed core radio spectra, suggesting an absorber on our line of sight at both optical and radio wavelengths.

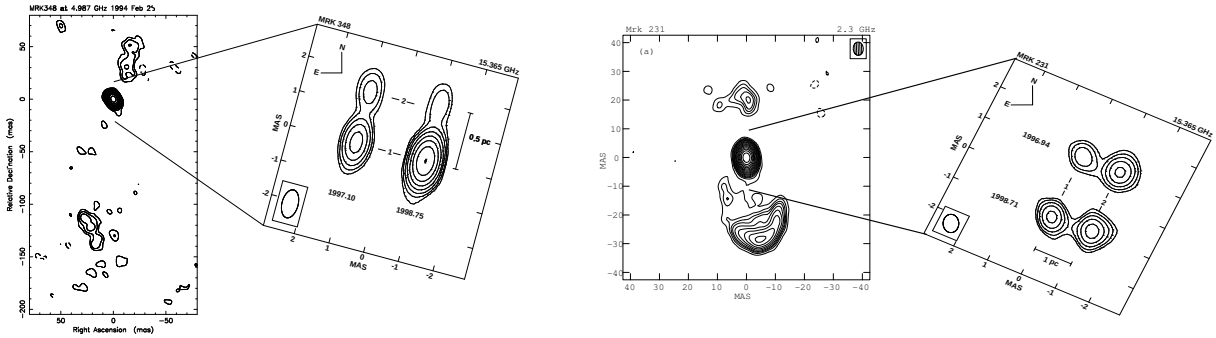

Figure 2: Jet motion in two Seyfert galaxies. Left: Mrk 348 imaged at 7.5×5.7 mas resolution with a Global VLBI array at 4.8 GHz ([14]). The core is shown at higher resolution (0.80×0.45 mas) imaged with the VLBA at 15 GHz at two epochs (1997.10 and 1998.75 [17]). Right: Mrk 231 imaged at 4.6×3.5 mas with the VLBA at 2.3 GHz (from [13]). The core is shown at higher resolution (0.7×0.5 mas) imaged with the VLBA at 15 GHz at two epochs (1996.94 and 1998.71 [17]). Motion between the nuclear components is detectable, yielding measurements of the jet speeds of (0.073 ± 0.035) mas yr^{-1} and (0.046 ± 0.017) mas yr^{-1}. The 15-GHz images are self-calibrated and the rms noise is 0.4-0.5 mJy beam^{-1} (except for the 2nd-epoch of Mrk 348 which had 1.1 mJy beam^{-1}).

3.3 Results 3: Jet Speeds

Active galaxies tend to be powerful or weak radio sources and though the dichotomy has been known for 30 years we still do not know its origin. Perhaps the engine is the same in both systems and the jet gets disrupted by dense interstellar medium in the radio-quiet objects (e.g. III Zw 2 [20]), or else the difference is intrinsic with jet power scaling with black hole spin [21, 22]. To distinguish, one could measure the jet speed close to the jet base, before environmental effects have become important.

We have observed Mrk 348 and Mrk 231 at two epochs with a 1.7-yr baseline, between late-1996/early-1997 and 1998 (Fig 2) [17], and have 18-cm observations of NGC 4151 at 20-mas resolution with the EVN in 1984 from the literature [8] and with the VLBA at 1996.5.

The nucleus of Mrk 348 is resolved into a double source whose component separation increased from 1.46 mas (0.46 pc) to 1.58 mas (0.50 pc) between the two epochs, yielding a proper motion of (0.073 ± 0.035) mas yr^{-1}. The nucleus of Mrk 231 is also resolved into a double, whose component separation increased from 1.08 mas (1.0 pc) to 1.16 mas (1.08 pc), yielding a proper motion of (0.046 ± 0.017) mas yr^{-1}. The nucleus of NGC 4151 is resolved into a triple source with component separations of 7 pc and 36 pc. No increase in the separations larger than 0.48 pc and 0.85 pc was found, corresponding to upper limits on the proper motion of 0.14 and 0.25 c. New VLBA data at higher resolution should soon measure the jet speed and spectral indices on sub-pc scales in NGC 4151.

In all three objects, the jet speeds are sub-relativistic, different from the high jet speeds seen in powerful radio sources (Fig 3), and at least two are sub-relativistic as they emerge from the broad-line region (BLR). This may be due to BLR gas on scales < 0.5 pc, or may be intrinsic due to black hole spin rate.

3.4 Results 4: Misaligned Jets

In Mrk 231, the parsec-scale jet is misaligned by 65° with the 40-pc-scale lobes in our 15-GHz VLBA image (Fig 4). Likewise, in NGC 4151, the sub-pc-scale jet is misaligned by 65° with the 300-pc-scale jet in our 4.8-GHz VLBA image. The bend in the jet occurs 0.8 pc from the core (Fig 4).

Bent jets are common in radio-loud objects, but those are probably projection effects caused by close alignment to our line of sight. But in these two Seyfert galaxies, the inclination to the line of sight is

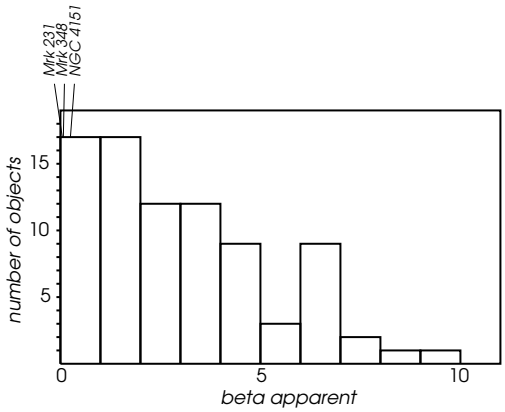

Figure 3: The distribution of jet speeds for a uniform sample of strong, flat-spectrum objects (comprised of quasars, BL Lac objects, galaxies, and empty fields [23]), and the speeds measured for the Seyferts Mrk 231, Mrk 348, and NGC 4151 shown for comparison. The Seyferts populate the slow end of the distribution. More Seyferts need to be observed to establish more firmly that their speeds are systematically low.

probably large [17], and the bends are probably intrinsic. A possible cause might be accretion-disc precession, perhaps by a mechanism as discussed by [25]; timescale for precession may be similar to that for the jet to propagate the 0.8 pc to the bend at 10000 km s^{-1} [24]. However, the once-only bend requires that such precession be only transient, and that the nucleus be located at the bend. The misalignment complicates standard unification schemes, in which the plane of the torus defines both the jet axis and the narrow-line region axis through shadowing, but may be reconciled if the inner disc defines the jet axis and the outer disc (dust torus) defines the shadowing axis, and the disc is warped.

3.5 Results 5: Free-Free Emission Search

We have conducted a search for further examples of thermal emission from the ionized inner edge of the accretion disc [26]. In the first four sources (T0109-383, NGC 2110, NGC 5252, Mrk 926) the nuclear source was detected but was unresolved by the VLBA, indicating $T_{\rm b}$ in excess of 10^8 K and sizes less than 1 pc. The emission is probably non-thermal and SSA in these galaxies. In one galaxy (NGC 2110) the emission was extended by ~ 0.2 pc along the direction of the 400-pc scale VLA jet, suggesting that the emission comes from the base of the jet. In NGC 4388, the flat-spectrum nuclear source was undetected by the VLBA at 8.4 GHz but was detected by MERLIN at 5 GHz. This infers 1.9×10^4 K $< T_{\rm b} < 10^6$ K, which is too low for SSA and may instead be optically-thin thermal emission from gas at $> 10^{4.5}$ K and $n_{\rm e} > 1.6 \times 10^4 f^{-0.5}$ cm^{-3}, where f is the volume filling factor. We are following up with VLBA observations at 1.4 GHz to resolve the emission region. Thus, this search found that NGC 4388 may produce thermal emission from the nucleus, like NGC 1068, and found no evidence for thermal disc-like emission extended perpendicular to the collimation axis in the other four galaxies.

4 Impact of The Square Kilometre Array (SKA)

The following highlights some Seyfert-related topics on which SKA would make a big impact.

4.1 Science

Thermal emission from the inner edge of the torus may have been seen in NGC 1068 [3], and a search of five further likely candidates found another possible example, NGC 4388. Its non-detection by the VLBA at 8.4 GHz infers low $T_{\rm b}$ and we now need more sensitivity like that of SKA to go further.

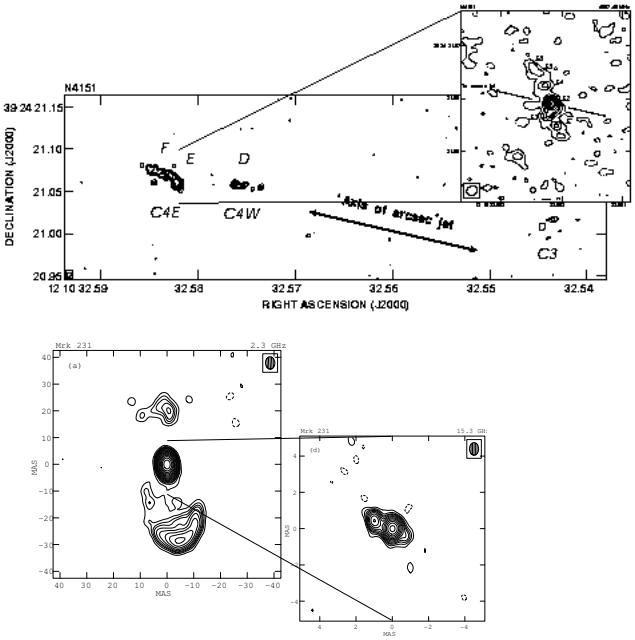

Figure 4: Top panel: NGC 4151 VLBA 18 & 6 cm (inset) images with 5.8×4.8 and 2.1×1.8 mas resolution [24]. Bottom panel: Mrk 231 VLBA 13 cm and 2 cm (inset) with 4.6×3.5 and 0.7×0.5 mas resolution [13]. Both objects show pc-scale jets that are misaligned with the larger-scale jets.

Ionized gas in the torus should generate radio recombination lines which, if detected, would allow one to map the gas dynamics closer to the black hole than do the water masers, and in many more systems than produce masers. Surveys for radio recombination lines from Seyfert and starburst galaxies have already shown that the emission line is weak, being only mJy at cm-wavelengths [27]. Radio recombination line observations with VLBI will be challenging and will demand sensitive arrays.

Free-free absorption measurements along the jet and the (presently undetected) counterjet will allow us to trace the distribution and density of ionized gas in the inner parsec, revealing whether the absorber is a torus or fills the nucleus, where the inner edge lies, whether the gas is smooth or clumpy, and perhaps revealing dense clouds that may be deflecting the jet. Clearer images of the jet could show whether the bends are sharp or gradual and show features due to collisions with dense clouds.

Jet speeds can now be measured for only a few of the brightest Seyferts, due to sensitivity limits, and speeds seem to be much less than those in powerful radio galaxies. To establish this result more firmly needs larger samples which means monitoring fainter galaxies than possible at present.

Polarimetry offers measurements of magnetic field strength and structure which is interesting for studying jet collimation and acceleration in Seyferts. But polarized flux is low in the few well-studied Seyferts. For the strongest, like NGC 1068, the limits on core polarization are $< 1\%$, but for most there are no good limits, only non-detections of polarization. To go further demands SKA-like sensitivity. With that, one might resolve structures transverse to the jets with the highest linear resolution of any type of AGN, since Seyferts are the the most numerous and hence nearest of the AGNs.

4.2 Imaging Performance

Weak sources (< 5 mJy for VLBA at 6 cm and 128 Mbps) cannot be self-calibrated because the SNR is $< \sqrt{2}$ on a single baseline within the atmospheric coherence time. Phase referencing must be used instead, but, whilst this permits the detection of weak sources, it incurs a loss of image fidelity and coherence and causes the appearance of spurious structure due to residual atmospheric scintillation. As an example, Fig 5 shows a typical case. In this test we observed with the VLBA at 15 GHz two geodetic calibrators, B1222+037 (410 mJy) and B1226+023 (3C273; 7.6 Jy), both good point sources, separated by $4.5°$, cycling between them with a 5-min cycle time, for three hours. After phase referencing from

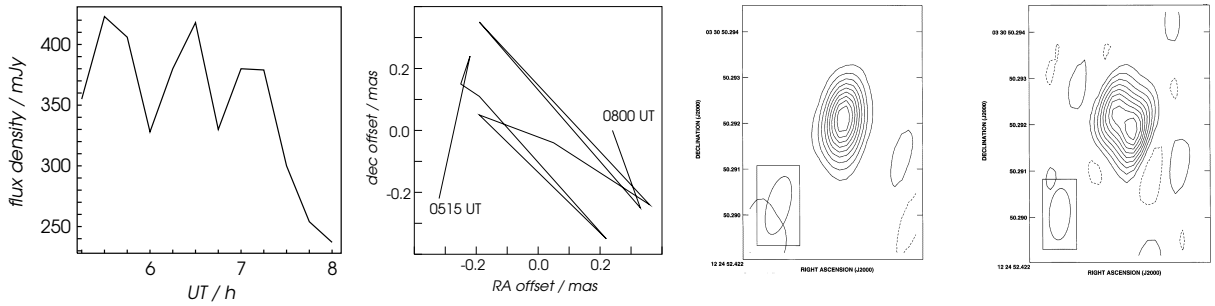

Figure 5: Test of phase referencing performance. a) Peak flux density in the phase-referenced image of B1222+037 vs time, for images made every 15 min. The source is probably constant to $< 1\%$ and the variability seen here is due to residual atmospheric scintillation. b) The position of the peak in the phase-referenced image of B1222+037 is shown for every 15 min interval throughout the 3-h experiment. Peak-to-peak motion is comparable to the beamwidth (1.5×0.5 mas). c) The phase-referenced image of B1222+037 produced from one 15-min snapshot. Peak brightness is 424 mJy beam^{-1} and the lowest contour is 10% of the peak. d) The phase-referenced image of B1222+037 produced from all 3 h of data. Apparent core-jet structure is caused by source motion due to residual atmospheric scintillation. Peak brightness is 283 mJy beam^{-1} and the lowest contour is 10% of the peak.

B1226+023 to image B1222+037, one should get a point source at the phase centre if all worked well. However, residual phase errors remain due to small differences in the atmosphere along the two lines of sight and probably due to errors in the correlator model. These cause spurious source structures, loss of coherence, source scintillation, and time-dependent shifts of the peak position.

Much better would be to use the sensitivity of SKA to enable self-cal on sources down to 0.09 mJy (assumes $\nu = 5$ GHz, $\Delta\nu = 512$ MHz, 1-bit sampling, $A_{\rm eff}/T_{\rm sys} = 9.20$ m^2 K^{-1} (where $A_{\rm eff}$ is the effective area) for each VLBA antenna and $A_{\rm eff}/T_{\rm sys} = 20000$ m^2 K^{-1} for the SKA, 300-s coherence time, 5-σ detection threshold), above which level the typical source separation is 2", and moderately large VLBI delay-rate beams can be expected to contain potential calibration sources.

4.3 Image Sensitivity

Fig 6 simulates the dramatic improvement in image quality that SKA should provide. At the left is a fairly good image of Mrk 348 (15 stations, global VLBI 1994, 6 cm, 1 h, 0.1 mJy rms), showing a strong core and some weak extended emission from jets that may be interacting with the narrow-line region gas [14]. Next is the classic 6-cm VLA image of Cyg A [28] to which has been added noise to degrade it until it 'looks' about the same as the Mrk 348 image. Last, the noise in the Cyg A image is reduced by a factor of 50, which is the amount by which the noise would be reduced by adding the SKA to the VLBA (assumes VLBA-only observes at 6 cm with 128-MHz bandwidth, 1-bit sampling, $A_{\rm eff}/T_{\rm sys} = 9.20$ m^2 K^{-1} per antenna , and VLBA+SKA observes at 6 cm with 512-MHz bandwidth, 1-bit sampling, $A_{\rm eff}/T_{\rm sys} = 9.20$ m^2 K^{-1} per VLBA antenna, and $A_{\rm eff}/T_{\rm sys} = 20000$ m^2 K^{-1} for SKA). The impact of SKA should be dramatic.

Acknowledgements

NRAO is a facility of the National Science Foundation operated under cooperative agreement by Associated Universities, Inc. We thank A.J.Beasley for supplying the phase referencing test data.

References

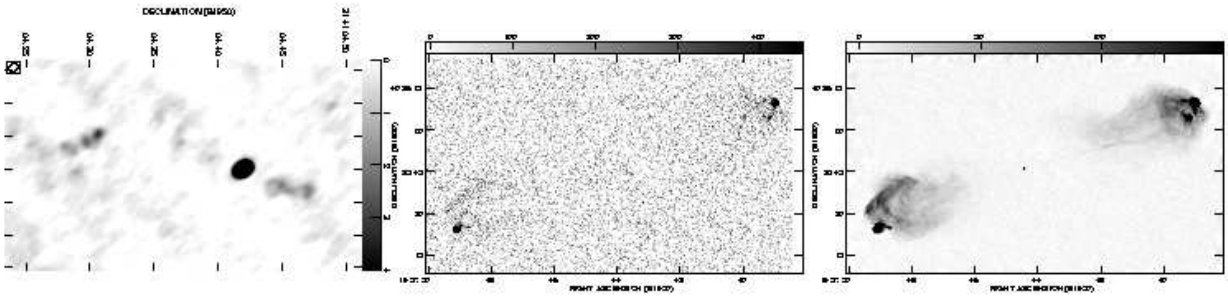

Figure 6: Left panel: Mrk 348 at 6 cm from a 15-station global VLBI observation [14]. Centre panel: Cyg A at 6 cm with the VLA [28], with noise added until it 'looks' like the Mrk 348 image. Right panel: As for the centre panel, but with the noise reduced by a factor of 50 as SKA would do if added into an array with the VLBA.

[1] M. Miyoshi, J. Moran, J. Herrnstein, L. Greenhill, N. Nakai, P. Diamond, & M. Inoue 1995, Nature, 373, 127
[2] L. Greenhill 1998, in *Radio Emission from Galactic and Extragalactic Compact Sources*, proc IAU Colloquium 164, eds. J. A. Zensus, G. B. Taylor, & J. M. Wrobel, p221
[3] J. F. Gallimore, S. A. Baum, & C. P. O'Dea 1997, Nature, 388, 852
[4] J. H. Krolik & S. Lepp 1989, ApJ, 347, 179
[5] D. A. Neufeld, P. R. Maloney & S. Conger 1994, ApJ, 436, L127
[6] J. H. Krolik & M. C. Begelman 1988, ApJ, 329, 702
[7] T. P. Krichbaum, W. Alef, A. Witzel, J. A. Zensus, R. S. Booth, A. Greve, & A. E. E. Rogers 1998, A&A, 329, 873
[8] B. Harrison, A. Pedlar, S. W. Unger, P. Burgess, D. A. Graham, E. Preuss 1986, MNRAS, 218, 775
[9] J. S. Ulvestad, & A. S. Wilson 1989, ApJ, 343, 659
[10] J. F. Gallimore, S. A. Baum, & C. P. O'Dea 1996, ApJ, 464, 198
[11] A. L. Roy, E. J. M. Colbert, A. S. Wilson & J. S. Ulvestad, 1998, ApJ, 504, 147
[12] A. S. Wilson, A. L. Roy, J. S. Ulvestad, E. J. M. Colbert, K. A. Weaver, J. A. Braatz, C. Henkel, M. Matsuoka, S. Xue, N. Iyomoto & K. Okada 1998, ApJ, 505, 587
[13] J. S. Ulvestad, J. M. Wrobel & C. L. Carilli 1999, ApJ, 516, 127
[14] T. P. Krichbaum, & A. L. Roy 1999, in preparation
[15] R. Barvainis, & C. Lonsdale 1998, AJ, 115, 885
[16] C. G. Mundell, A. Pedlar, S. A. Baum, C. P. O'Dea, J. F. Gallimore, E. Brinks 1995, MNRAS, 272, 355
[17] J. S. Ulvestad, J. M. Wrobel, A. L. Roy, A. S. Wilson, H. Falcke & T. P. Krichbaum 1999, ApJ, 517, L81
[18] D. A. Smith & C. Done 1996, MNRAS, 280, 355
[19] T. Nakagawa et al. 1997, IAU Symp 186, Galaxy Interactions at Low and High Redshift, p103
[20] H. Falcke et al. 1999, ApJ, 514, L17
[21] M. J. Rees, E. S. Phinney, M. C. Begelman, & R. D. Blandford 1982, Nature, 295, 17
[22] A. S. Wilson & E. J. M. Colbert 1995, ApJ, 438, 62
[23] R. C. Vermeulen 1995, Proc Natl Acad Sci USA, 92, 11385
[24] J. S. Ulvestad, A. L. Roy, E. J. M. Colbert & A. S. Wilson 1998, ApJ, 496, 196
[25] J. M. Pringle 1997, MNRAS, 292, 136
[26] C. G. Mundell, A. S. Wilson, J. S. Ulvestad, & A. L. Roy 1999, ApJ, (submitted)
[27] K. R. Anantharamaiah, J.-H. Zhao, W. M. Goss, & F. Viallefond 1993, ApJ, 419, 585
[28] R. A. Perley, J. W. Dreher, & J. J. Cowan 1984, ApJ, 285, L35